RAA 2018 Vol. **18** No. **3**, 30(6pp) doi: 10.1088/1674–4527/18/3/30

http://www.raa-journal.org *http://iopscience.iop.org/raa*

Research in Astronomy and Astrophysics

First photometric study of ultrashort-period contact binary 1SWASP J140533.33+114639.1

Bin Zhang[1,2,3], Sheng-Bang Qian[1,2,3], Ri Michel[4], Boonrucksar Soonthornthum[5] and Li-Ying Zhu[1,2,3]

[1] Yunnan Observatories, Chinese Academy of Sciences, Kunming 650216, China; *zhangbin@ynao.ac.cn*
[2] Key Laboratory of the Structure and Evolution of Celestial Objects, Chinese Academy of Sciences, Kunming 650216, China
[3] University of Chinese Academy of Sciences, Beijing 100049, China
[4] Instituto de Astronomía, UNAM, Ensenada, México
[5] National Astronomical Research Institute of Thailand, Chiang Mai 50200, Thailand

Received 2017 November 7; accepted 2017 December 25

Abstract In this paper, CCD photometric light curves for the short-period eclipsing binary 1SWASP J140533.33+114639.1 (hereafter J1405) in the BVR bands are presented and analyzed using the 2013 version of the Wilson-Devinney (W-D) code. It is discovered that J1405 is a W-subtype shallow contact binary with a contact degree of $f = 7.9 \pm 0.5\%$ and a mass ratio of $q = 1.55 \pm 0.02$. In order to explain the asymmetric light curves of the system, a cool starspot on the more massive component is employed. This shallow contact eclipsing binary may have been formed from a short-period detached system through orbital shrinkage due to angular momentum loss. Based on the $(O - C)$ method, the variation of orbital period is studied using all the available times of minimum light. The $(O - C)$ diagram reveals that the period is increasing continuously at a rate of $dP/dt = +2.09 \times 10^{-7}\,\mathrm{d\,yr^{-1}}$, which can be explained by mass transfer from the less massive component to the more massive one.

Key words: stars: binaries: close — stars: binaries: eclipsing — stars: individual (1SWASP J140533.33+114639.1)

1 INTRODUCTION

W UMa type contact binaries exhibit a sharp period cut-off phenomenon around 0.22 days (Rucinski 1992). A recent study using data released by the Large Sky Area Multi-Object Fiber Spectroscopic Telescope (LAMOST) found that the updated value is around 0.2 days (Qian et al. 2017). Ultrashort-period (less than 0.23 days) contact eclipsing binaries (EBs) are important for modern astrophysics: (1) they can be utilized to detect the distance of stars by relying on their empirical period-luminosity relation (Rucinski 2004); (2) these binaries offer significant information about origin and evolution of late-type stars including mass and angular momentum loss (AML), and even the merging (Qian et al. 2014; Kjurkchieva et al. 2016). With the development of technology, more and more contact EBs with short-periods have been discovered by some sky surveys around the world (e.g., SDSS, SuperWASP and NSVS). Till now, some of them have been studied in detail, such as CC Com (Köse et al. 2011; Yang & Liu 2003), GSC 1387–475 (Rucinski & Pribulla 2008), 1SWASP J015100.23-100524.2 (Qian et al. 2015b), NSVS 4484038 (Zhang et al. 2014) and the stable red-dwarf contact binary SDSS J001641-000925 (Davenport et al. 2013; Qian et al. 2015a).

1SWASP J140533.33+114639.1 (hereafter J1405), as a short-period contact EB candidate with an orbital period of about 0.225123 days, was first detected in 2013 (Lohr et al. 2013). Its light curves (LCs) present characteristics of a typical EW-type (nearly equal light minima). The Two Micron All Sky Survey (2MASS, Cutri et al. 2003) provides its magnitude of V=15.51, J=14.019, H=13.487 and K=13.328, and the corresponding color indexes are $V - K$=2.182, $J - H$=0.532

Table 1 Coordinates of J1405, and the Comparison and Check Stars

Stars	$\alpha_{\rm J2000}$	$\delta_{\rm J2000}$
J1405	$14^{\rm h}05^{\rm m}33.33^{\rm s}$	$11^\circ46'39.1''$
Comparison	$14^{\rm h}05^{\rm m}38.23^{\rm s}$	$11^\circ41'17.3''$
Check	$14^{\rm h}05^{\rm m}59.16^{\rm s}$	$11^\circ40'38.3''$

and $H-K$=0.159 for the system, which imply an average spectral type of about K4. However, there is no spectroscopic element, photometric solution or period research published until now. In the present paper, the LCs are analyzed using the Wilson-Devinney (W-D) program and its photometric solutions are obtained. All times of minimum light are collected and the period variations are analyzed. The evolutionary scenario and magnetic activity are also discussed.

2 MULTI-COLOR CCD PHOTOMETRIC OBSERVATIONS

Photometric observations of J1405 were carried out on 2016 March 17 and 22 utilizing the 84 cm telescope at the Observatorio Astronómico Nacional (OAN) in Sierra San Pedro Mártir, Mexico. This relatively small telescope is mainly employed for photometric observations, because more than 60% of the nights at this site have photometric quality (Tapia 2003). The integration times for each image in BVR bands were 70 s, 40 s and 25 s, respectively. All the observed images were reduced using the aperture photometric package PHOT of IRAF by Mr. Michel. Another two stars near the target were chosen as the comparison star and check star. The coordinates of the variable star, comparison star and check star are listed in Table 1. Two sets of LCs obtained are plotted in Figure 1. The LCs are asymmetric and show a weak O'Connell effect (O'Connell 1951), where the maxima following the primary minima are higher than the other maxima. The average observational errors and the amplitudes of light variation in different bands are listed in Table 2.

Meanwhile, some new times of light minimum for J1405 were also observed and determined using the least-squares parabolic fitting method. By applying the following linear ephemeris

$$\begin{aligned}\mathrm{Min.(HJD)} =& 2457466.00294(\pm0.00019)\\ &+ 0.225123^{\rm d} \times E\,,\end{aligned} \tag{1}$$

the $(O-C)$ values and observational LCs' phase were calculated. The zeropoint displayed in this linear ephemeris was one of the primary eclipse times, which was determined with observed data from the 84 cm telescope, and the orbital period we adopted came from the SuperWASP EB catalog (Lohr et al. 2013). All the minima times and their corresponding $(O-C)$ values are listed in Table 3.

3 ORBITAL PERIOD INVESTIGATION

The $(O-C)$ method is the traditional way to reveal variations in orbital period. Before the present work, only one minimum time of J1405 had been published. For analyzing the period changes of the system, we collected all the CCD times of light minima. Mr. Marcus Lohr sent us 121 minima times from SuperWASP, and the LCs obtained from OAN offered another 4. Minima times with the same epoch have been averaged, and only the mean values are listed in Table 3. In our fitting process, according to determined errors listed in Table 3, the weight of the SuperWASP data is 1 and that of our data is 5.

The $(O-C)$ diagram shows a upward parabolic variation and the fitting curve is plotted in Figure 2. Based on the least-squares method, the new ephemeris

$$\begin{aligned}\mathrm{Min.\ I} \;=\; & 2457470.95618(\pm0.0003)\\ &+0.22512639^{\rm d}(\pm0.00000003)\times E\\ &+1.29(\pm0.02)\times10^{-10}\times E^2\,,\end{aligned} \tag{2}$$

was obtained. With the quadratic term included in this equation, a secular period increase rate is determined to be $dP/dt = 2.09\times10^{-7}\,\mathrm{d\,yr^{-1}}$.

4 PHOTOMETRIC SOLUTIONS

To derive its physical parameters, the 2013 version of the W-D program (Wilson & Devinney 1971; Wilson & Van Hamme 2003; Wilson et al. 2010) is utilized. The numbers of observational data applied in the program are 81 in the B band, 78 in the V band and 72 in the R band.

Before analyzing the LCs, the values of some input parameters were set. The temperature for star 1 (star eclipsed at the primary light minimum), $T_1 = 4680$ K, was fixed according to mean color index (Cox 2000). We took the same values of gravity-darkening coefficients and bolometric albedo for both components, i.e., $g_1 = g_2 = 0.32$ according to the stellar temperatures given by Claret (2000) and $A_1 = A_2 = 0.5$ (Lu & Rucinski 1993) were set for late-type stars with a convective envelope. The bolometric and bandpass limb-darkening coefficients were chosen from van Hamme

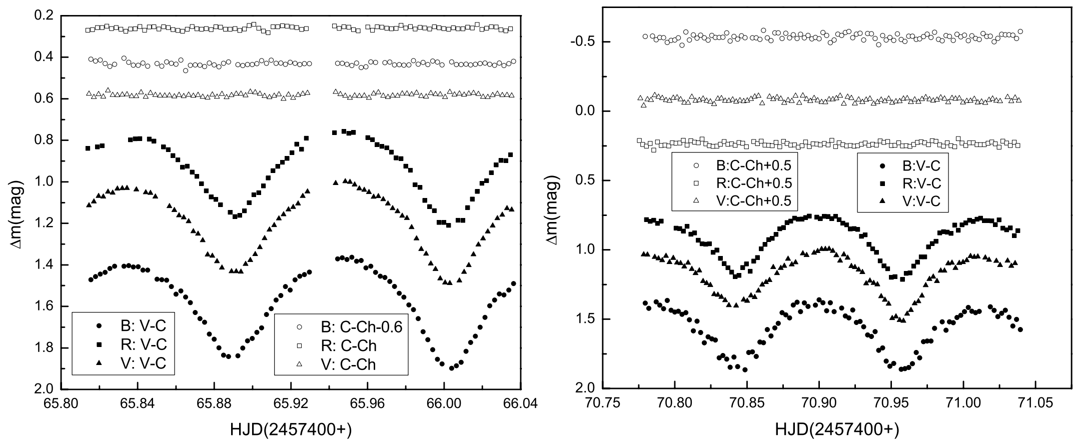

Fig. 1 The observational LCs of J1405 in BVR bands. The differential LCs of the comparison star relative to the check star are also plotted.

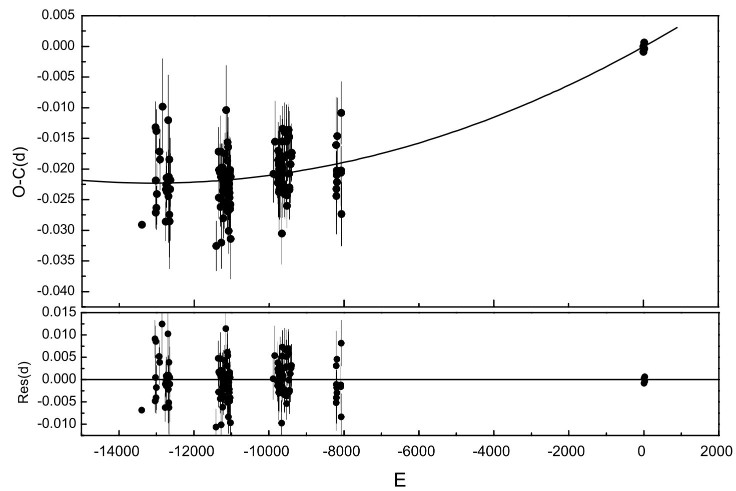

Fig. 2 The $(O - C)$ diagram of J1405 formed by all available measurements. The $(O - C)$ values were computed by using a newly determined linear ephemeris (Eq. (1)). The *solid line* represents the quadratic fit (Eq. (2)). The *bottom panel* plots residuals for Eq. (2).

Table 2 Average Observational Errors and Amplitudes of Light Variation in March 2016

Band	Date	Error (mag)	Δm (mag)	Date	Error (mag)	Δm (mag)
B	17	0.0071	0.5852	22	0.0102	0.6646
V	17	0.0071	0.5231	22	0.0087	0.5592
R	17	0.0067	0.5480	22	0.0081	0.5303

(1993). To account for the limb-darkening in detail, logarithmic functions were used. These fixed parameters are listed in Table 4. The adjustable parameters were: mass ratio, q; orbital inclination, i; mean temperature of star 2, T_2; dimensionless potentials of the two components Ω_1 and Ω_2; monochromatic light of star 1, L_{1B}, L_{1V} and L_{1R}.

Two sets of LCs were obtained, but the data from March 17 have better quality. So, we started the analysis with this set of LCs. Mode 3 for a contact binary system is adopted ($\Omega_1 = \Omega_2$ in this case). Because there are no spectroscopic observations for J1405 published, we apply a q-search method (with fixed q) to obtain initial input parameters. The solutions are carried out with mass ratios ranging from less than 0.25 to larger than 3.0. The relation between the sum of weighted square deviations $\Sigma\omega(O-C)^2$ and q is plotted in Figure 3. Values of $\Sigma - q$ exhibit their lowest value at $q = 1.55$. We then set the

Table 3 $(O-C)$ Values of Light Minima for J1405

HJD (2450000+)	$(O-C)$	E	Filter	Telescope	HJD (2450000+)	$(O-C)$	E	Filter	Telescope	HJD (2450000+)	$(O-C)$	E	Filter	Telescope
7465.8895(02)	−0.0009	−0.5	BVR	84 cm	4941.4512(46)	−0.0224	−11214	V	INGT	5279.5906(0.40)	−0.0178	−9712	V	INGT
7466.0029(02)	0.0000	0	BVR	84 cm	4942.5783(57)	−0.0209	−11209	V	INGT	5280.4858(0.49)	−0.0230	−9708	V	INGT
7470.8427(08)	−0.0004	21.5	BVR	84 cm	4943.4743(43)	−0.0254	−11205	V	INGT	5281.6167(0.65)	−0.0178	−9703	V	INGT
7470.9563(06)	0.0006	22	BVR	84 cm	4944.6026(31)	−0.0228	−11200	V	INGT	5290.6089(0.50)	−0.0305	−9663	V	INGT
4450.0010(...)	−0.0291	−13397	V	INGT	4945.5019(30)	−0.0239	−11196	V	INGT	5291.5206(0.44)	−0.0193	−9659	V	INGT
4530.6109(42)	−0.0132	−13039	V	INGT	4949.5605(34)	−0.0175	−11178	V	INGT	5292.6417(0.42)	−0.0238	−9654	V	INGT
4532.6232(26)	−0.0271	−13030	V	INGT	4950.4561(26)	−0.0224	−11174	V	INGT	5293.5505(0.36)	−0.0155	−9650	V	INGT
4533.5289(49)	−0.0218	−13026	V	INGT	4955.6460(73)	−0.0104	−11151	V	INGT	5294.6693(0.24)	−0.0223	−9645	V	INGT
4535.5631(35)	−0.0138	−13017	V	INGT	4963.5170(47)	−0.0187	−11116	V	INGT	5295.5787(0.37)	−0.0134	−9641	V	INGT
4536.4510(35)	−0.0263	−13013	V	INGT	4964.6351(39)	−0.0262	−11111	V	INGT	5297.5974(0.49)	−0.0208	−9632	V	INGT
4539.6050(50)	−0.0241	−12999	V	INGT	4965.5461(59)	−0.0157	−11107	V	INGT	5298.4989(0.32)	−0.0198	−9628	V	INGT
4555.5957(21)	−0.0171	−12928	V	INGT	4966.6605(48)	−0.0269	−11102	V	INGT	5304.5789(0.41)	−0.0181	−9601	V	INGT
4558.5209(50)	−0.0185	−12915	V	INGT	4967.5715(48)	−0.0164	−11098	V	INGT	5307.4995(0.37)	−0.0241	−9588	V	INGT
4573.6128(78)	−0.0098	−12848	V	INGT	4968.4678(39)	−0.0205	−11094	V	INGT	5308.6352(0.48)	−0.0140	−9583	V	INGT
4591.6039(32)	−0.0286	−12768	V	INGT	4969.5905(47)	−0.0235	−11089	V	INGT	5309.5267(0.51)	−0.0230	−9579	V	INGT
4593.6353(27)	−0.0233	−12759	V	INGT	4970.4921(36)	−0.0224	−11085	V	INGT	5318.5369(0.82)	−0.0178	−9539	V	INGT
4596.5626(37)	−0.0226	−12746	V	INGT	4971.6100(37)	−0.0301	−11080	V	INGT	5319.6648(0.37)	−0.0155	−9534	V	INGT
4597.4642(43)	−0.0214	−12742	V	INGT	4972.5159(55)	−0.0247	−11076	V	INGT	5321.4552(0.36)	−0.0260	−9526	V	INGT
4598.5876(41)	−0.0237	−12737	V	INGT	4973.6431(43)	−0.0232	−11071	V	INGT	5322.5825(0.36)	−0.0243	−9521	V	INGT
4608.5046(74)	−0.0121	−12693	V	INGT	4974.5450(49)	−0.0217	−11067	V	INGT	5324.6152(0.42)	−0.0177	−9512	V	INGT
4609.6179(76)	−0.0244	−12688	V	INGT	4975.6699(22)	−0.0224	−11062	V	INGT	5331.5982(0.37)	−0.0136	−9481	V	INGT
4611.6472(33)	−0.0212	−12679	V	INGT	4976.5682(57)	−0.0247	−11058	V	INGT	5333.6231(0.54)	−0.0147	−9472	V	INGT
4613.6671(69)	−0.0274	−12670	V	INGT	4977.4694(50)	−0.0239	−11054	V	INGT	5334.5176(0.35)	−0.0207	−9468	V	INGT
4614.5766(69)	−0.0184	−12666	V	INGT	4978.5984(58)	−0.0205	−11049	V	INGT	5335.6492(0.41)	−0.0147	−9463	V	INGT
4615.4670(77)	−0.0286	−12662	V	INGT	4979.4993(52)	−0.0201	−11045	V	INGT	5336.5411(0.36)	−0.0234	−9459	V	INGT
4619.5244(84)	−0.0233	−12644	V	INGT	4980.6185(36)	−0.0265	−11040	V	INGT	5337.6671(0.52)	−0.0230	−9454	V	INGT
4620.6515(43)	−0.0218	−12639	V	INGT	4981.5197(53)	−0.0258	−11036	V	INGT	5343.5241(0.63)	−0.0192	−9428	V	INGT
4896.6416(41)	−0.0326	−11413	V	INGT	4982.6499(35)	−0.0213	−11031	V	INGT	5348.4781(0.39)	−0.0179	−9406	V	INGT
4910.6146(40)	−0.0172	−11351	V	INGT	4983.5402(65)	−0.0314	−11027	V	INGT	5350.5047(0.47)	−0.0174	−9397	V	INGT
4912.6332(34)	−0.0247	−11342	V	INGT	5240.6413(47)	−0.0208	−9885	V	INGT	5617.5019(0.78)	−0.0161	−8211	V	INGT
4913.5382(32)	−0.0202	−11338	V	INGT	5249.6515(66)	−0.0155	−9845	V	INGT	5618.6192(0.62)	−0.0244	−8206	V	INGT
4919.6161(47)	−0.0206	−11311	V	INGT	5265.6296(35)	−0.0212	−9774	V	INGT	5619.5208(0.57)	−0.0232	−8202	V	INGT
4921.6366(32)	−0.0262	−11302	V	INGT	5267.6546(35)	−0.0223	−9765	V	INGT	5620.6495(0.27)	−0.0202	−8197	V	INGT
4923.6640(38)	−0.0249	−11293	V	INGT	5268.5603(32)	−0.0170	−9761	V	INGT	5621.5492(0.39)	−0.0210	−8193	V	INGT
4924.5722(59)	−0.0172	−11289	V	INGT	5269.4593(62)	−0.0185	−9757	V	INGT	5622.6737(0.34)	−0.0221	−8188	V	INGT
4925.4686(53)	−0.0213	−11285	V	INGT	5270.5812(39)	−0.0223	−9752	V	INGT	5623.5817(0.62)	−0.0146	−8184	V	INGT
4926.5957(39)	−0.0198	−11280	V	INGT	5271.4820(59)	−0.0219	−9748	V	INGT	5646.5382(0.54)	−0.0206	−8082	V	INGT
4927.4840(43)	−0.0320	−11276	V	INGT	5272.6103(38)	−0.0193	−9743	V	INGT	5647.6642(0.40)	−0.0202	−8077	V	INGT
4935.6006(39)	−0.0198	−11240	V	INGT	5273.5063(61)	−0.0238	−9739	V	INGT	5648.5741(0.51)	−0.0109	−8073	V	INGT
4936.4974(38)	−0.0235	−11236	V	INGT	5275.5328(48)	−0.0234	−9730	V	INGT	5649.4581(0.52)	−0.0274	−8069	V	INGT
4938.5190(33)	−0.0280	−11227	V	INGT	5276.6617(39)	−0.0200	−9725	V	INGT	6736.7630(0.02)	0.0460	−3239.5	V	INGT
4939.6506(34)	−0.0220	−11222	V	INGT	5277.5637(55)	−0.0185	−9721	V	INGT	6736.8722(0.03)	0.0426	−3239	V	INGT
4940.5518(40)	−0.0213	−11218	V	INGT	5278.4612(31)	−0.0215	−9717	V	INGT					

Ref: INGT means Isaac Newton Group of Telescopes, Apartado de Correos 321, E-38700 Santa Cruz de La Palma, Tenerife, Spain.

initial value of q to be 1.55 and treat it as an adjustable parameter. After all the free parameters converge, one set of solutions is derived. Because our LCs are asymmetric, and the main reason for this result is the variation of spot location and size (Kang et al. 2002). Considering this case, the cool starspot model was used to obtain better solutions. As is well known, four parameters can be used to describe a spot, namely the temperature, T_s; latitude, *Lat*; longitude *Lon* and angular radius *Rad*. During our analysis, only T_s was fixed in a series of trial values until we identified the best solution. Finally, we found that one cool starspot on the secondary component could yield the best fit, and the fitting residual of our solution with a spot is much smaller than that without a spot. Therefore, we adopted the cool starspot model as the final solution. The derived photometric solutions are listed in Table 5 and the theoretical LCs computed with the cool starspot model are plotted in Figure 4. Furthermore, we also derive the geometrical structure of the system, which is shown in Figure 5. Because the LCs obtained on March 22 have worse quality, we did not analyze them.

5 DISCUSSIONS AND CONCLUSIONS

The asymmetry displayed by the observed LCs suggests there is spot activity in the system. Therefore, we analyzed the LCs and obtained the photometric solutions with a cool starspot on the more massive component using the 2013 version of the W-D code. The results suggest that J1405 is a W-subtype contact EB near the short-

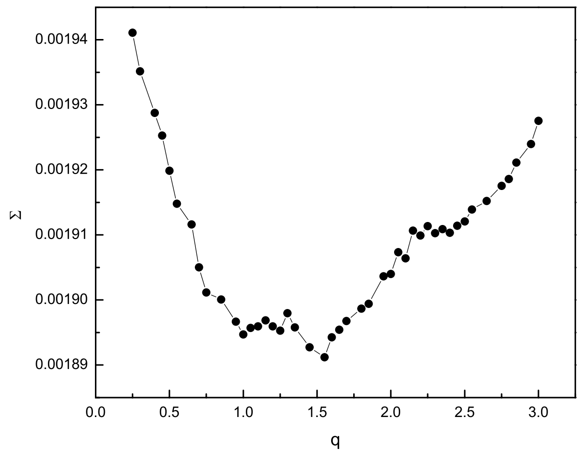

Fig. 3 The $\Sigma - q$ curve for J1405. The minimum for residuals is at $q = 1.55$.

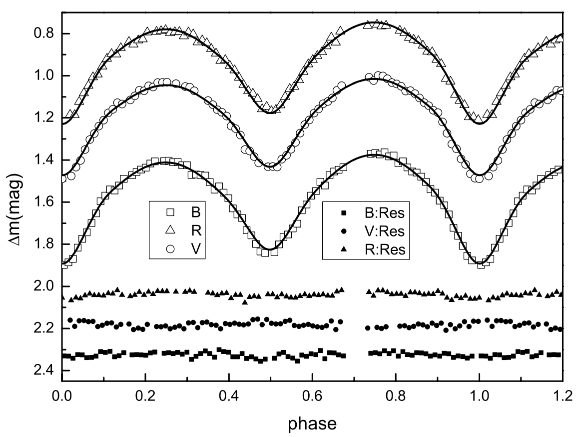

Fig. 4 Observed (*open circles*, *triangles* and *squares*) and theoretical LCs (*solid lines*) calculated with the cool starspot parameters listed in Table 5. Residuals from the solutions are shown in the *bottom panel*.

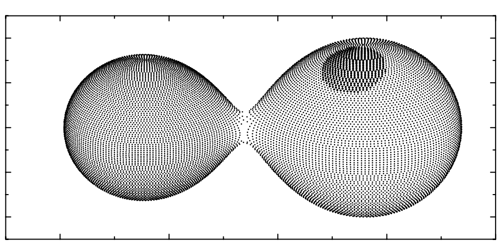

Fig. 5 Geometric structure of J1405 at phase 0.25.

Table 4 Fixed Parameters During Photometric Analysis

Parameter	Value
$g_1 = g_2$	0.32
$A_1 = A_2$	0.50
$x_{1\mathrm{bolo}}, x_{2\mathrm{bolo}}$	0.641, 0.638
$y_{1\mathrm{bolo}}, y_{2\mathrm{bolo}}$	0.172, 0.163
x_{1B}, x_{2B}	0.848, 0.844
y_{1B}, y_{2B}	0.096, 0.129
x_{1V}, x_{2V}	0.802, 0.801
y_{1V}, y_{2V}	0.045, 0.022
x_{1R}, x_{2R}	0.749, 0.755
y_{1R}, y_{2R}	0.123, 0.108

Table 5 Photometric Solutions for J1405

Parameter	March 17th No spot	Errors	March 17th With spot	Errors
T_1 (K)	4680	Assumed	4680	Assumed
q	1.5501	± 0.0199	1.5488	± 0.0163
T_2 (K)	4563	± 16	4523	± 21
i (°)	68.996	± 0.257	68.616	± 0.321
$L_1/(L_1+L_2)(B)$	0.4545	± 0.0074	0.4742	± 0.0135
$L_1/(L_1+L_2)(V)$	0.4434	± 0.0058	0.4590	± 0.0121
$L_1/(L_1+L_2)(R)$	0.4342	± 0.0045	0.4466	± 0.0112
Ω_1=Ω_2	4.5612	± 0.0092	4.5528	± 0.0026
r_1 (pole)	0.3237	± 0.0009	0.3247	± 0.0011
r_1 (side)	0.3391	± 0.0011	0.3402	± 0.0015
r_1 (back)	0.3733	± 0.0016	0.3751	± 0.0022
r_2 (pole)	0.3967	± 0.0009	0.3976	± 0.0014
r_2 (side)	0.4201	± 0.0011	0.4213	± 0.0018
r_2 (back)	0.4510	± 0.0015	0.4526	± 0.0025
f (%)	6.7	± 1.6	7.9	± 0.5
Latitude (°)			334.392	± 4.242
Longitude (°)			253.902	± 6.187
Radius (radian)			0.356	± 0.089
T_s			0.85	Assumed
$\sum \omega_i(O-C)_i^2$	0.001891		0.001135	

period cutoff with a mass ratio of q = 1.55 ± 0.02. The mean contact degree ($f = 7.3\,\%$) reveals that it is a shallow contact system with similar surface temperature of the components ($\Delta T = 140\,\mathrm{K}$). Similar contact binaries include AH Vir (Lu & Rucinski 1993; Kjurkchieva et al. 2015), RZ Com (He & Qian 2008; Xiang & Zhou 2004), AM Leo (Hiller et al. 2004), U Peg (Mohajerani & Percy 2011; Djurašević et al. 2001) and SW Lac (Şenavcı 2012). W UMa-type binaries are formed from initially detached binaries by AML via magnetic braking (Qian et al. 2013). Like other late K-type contact binaries with short periods, J1405 is also in marginal contact and presents remarkably asymmetric LCs, representing probable surface activities (Zhang et al. 2014; Jiang et al. 2015a). Just as Qian et al. (2015b) discussed, the orbital shrinkage due to AML may result in the formation of a contact system similar to J1405. The progenitor of J1405 may be a short-period detached EB system similar to DV Psc (Pi et al. 2014), and J1405 may be at the same evolutional phase as 1SWASP J015100.23-100524.2 (Qian et al. 2015b).

Another feature of J1405 is its spot activity. Generally, for late-type contact binary stars, their deep convective envelope along with fast rotation can help to produce a strong magnetic dynamo, thus they will display some solar-like activity such as photospheric cool starspots (Li et al. 2015). A cool starspot is known to be a strong magnetic area which can change the shape of LCs. We adopted the cool starspot model in the W-D program with one spot on the secondary component to explain it. Just as Figure 4 shows, the fitted LCs with a cool starspot coincides very well with the observational data at all phases. Therefore, using the cool starspot model to explain the asymmetry of LCs is reasonable.

Based on analysis of the $(O - C)$ diagram, we found that the orbital period of J1405 shows an upward parabolic variation, which represents an increase of the period. According to the obtained parameters, the rate of $dP/dt = 2.09 \times 10^{-7}\,\mathrm{d\,yr^{-1}}$ is derived. The secular increase of the orbital period may be interpreted as mass transfer from the less massive component to the more massive one, such as EP And (Liao et al. 2013), 1SWASP J074658.62+224448.5 (Jiang et al. 2015a) and 1SWASP J075102.16+342405.3 (Jiang et al. 2015b). However, the time span of our data is only 10 years, and the increase of period might be only a part of long-term changes. Further observations are required to confirm this result.

Acknowledgements This work is partly supported by the National Natural Science Foundation of China (Nos. 11133007 and 11573063) and the Science Foundation of Yunnan Province (Grant No. 2012HC011). Many thanks go to Dr. Marcus Lohr for his kind assistance sending us eclipse timings of J1405. We are also especially indebted to the anonymous referees who provided useful comments and cordial suggestions, which helped us to improve the paper greatly.

References

Cox, A. N. 2000, Allen's Astrophysical Quantities, ed. A. N. Cox (4th ed., New York: AIP Press; Springer), 1
Claret, A. 2000, A&A, 361, 1081
Cutri, R. M., Skrutskie, M. F., van Dyk, S., et al. 2003, VizieR Online Data Catalog, 2246
Davenport, J. R. A., Becker, A. C., West, A. A., et al. 2013, ApJ, 764, 62
Djurašević, G., Rovithis-Livaniou, H., Rovithis, P., Erkapić, S., & Milovanović, N. 2001, A&A, 367, 840
He, J.-J., & Qian, S.-B. 2008, ChJAA (Chin. J. Astron. Astrophys.), 8, 465
Hiller, M. E., Osborn, W., & Terrell, D. 2004, PASP, 116, 337
Jiang, L.-Q., Qian, S.-B., Zhang, J., & Zhou, X. 2015a, AJ, 149, 169
Jiang, L., Qian, S.-B., Zhang, J., & Liu, N. 2015b, PASJ, 67, 118
Kang, Y. W., Oh, K.-D., Kim, C.-H., et al. 2002, MNRAS, 331, 707
Kjurkchieva, D. P., Dimitrov, D. P., & Ibryamov, S. I. 2015, RAA (Research in Astronomy and Astrophysics), 15, 1493
Kjurkchieva, D., Popov, V., Vasileva, D., & Petrov, N. 2016, Serbian Astronomical Journal, 192, 21
Köse, O., Kalomeni, B., Keskin, V., Ulaş, B., & Yakut, K. 2011, Astronomische Nachrichten, 332, 626
Li, K., Hu, S.-M., Guo, D.-F., et al. 2015, AJ, 149, 120
Liao, W.-P., Qian, S.-B., Li, K., et al. 2013, AJ, 146, 79
Lohr, M. E., Norton, A. J., Kolb, U. C., et al. 2013, A&A, 549, A86
Lu, W.-X., & Rucinski, S. M. 1993, AJ, 106, 361
Mohajerani, S., & Percy, J. R. 2011, Journal of the American Association of Variable Star Observers (JAAVSO), 39, 80
O'Connell, D. J. K. 1951, MNRAS, 111, 642
Pi, Q.-f., Zhang, L.-Y., Li, Z.-m., & Zhang, X.-l. 2014, AJ, 147, 50
Qian, S.-B., Liu, N.-P., Li, K., et al. 2013, ApJS, 209, 13
Qian, S.-B., Jiang, L.-Q., Zhu, L.-Y., et al. 2014, Contributions of the Astronomical Observatory Skalnate Pleso, 43, 290
Qian, S.-B., Jiang, L.-Q., Fernández Lajús, E., et al. 2015a, ApJ, 798, L42
Qian, S. B., Zhang, B., Soonthornthum, B., et al. 2015b, AJ, 150, 117
Qian, S.-B., He, J.-J., Zhang, J., et al. 2017, RAA (Research in Astronomy and Astrophysics), 17, 087
Rucinski, S. M. 1992, AJ, 103, 960
Rucinski, S. M. 2004, New Astron. Rev., 48, 703
Rucinski, S. M., & Pribulla, T. 2008, MNRAS, 388, 1831
Şenavcı, H. V. 2012, in IAU Symposium, 282, From Interacting Binaries to Exoplanets: Essential Modeling Tools, eds. M. T. Richards, & I. Hubeny, 496
Tapia, M. 2003, in Revista Mexicana de Astronomia y Astrofisica, 27, eds. I. Cruz-Gonzalez, R. Avila, & M. Tapia, 75
van Hamme, W. 1993, AJ, 106, 2096
Wilson, R. E., & Devinney, E. J. 1971, ApJ, 166, 605
Wilson, R., & Van Hamme, W. 2003, Computing Binary Star Observables (the 4th edition of the W-D program)
Wilson, R. E., Van Hamme, W., & Terrell, D. 2010, ApJ, 723, 1469
Xiang, F. Y., & Zhou, Y. C. 2004, New Astron., 9, 273
Yang, Y., & Liu, Q. 2003, PASP, 115, 748
Zhang, X. B., Deng, L. C., Wang, K., et al. 2014, AJ, 148, 40